



Improvement of surface processes modelling in the ERO code

M.I. Airila^{a,*}, T. Ikonen^a, D. Borodin^b, A. Kirschner^b, K. Nordlund^c, A. Loarte^d

^a Association Euratom-Tekes, TKK Helsinki University of Technology, Espoo, Finland

^b Association Euratom-FZJ, IEF-4, Forschungszentrum Jülich, Trilateral Euregio Cluster, Germany

^c Association Euratom-Tekes, Accelerator Laboratory, University of Helsinki, Finland

^d EFDA CSU Garching, Boltzmannstrasse 2, Garching, Germany

ARTICLE INFO

PACS:

52.40.Hf
52.65.Cc
52.65.Pp
52.65.Yy

ABSTRACT

The low-impact-energy range of the data set used by the 3D Monte Carlo impurity transport code ERO has been supplemented by sputtering data calculated by molecular dynamics. Also reflection data for normal incidence were obtained. The computed sputtering data can be reasonably well fitted using the Bohdansky formula, yielding rather similar fitting parameter values to those used in ERO. A previously modelled case for ITER divertor has been simulated with the new data. As expected from the small change in the data set, the modelling results change only little. A method was also developed for direct coupling of ERO and the molecular dynamics code HCParcas, but the directly coupled code is not applicable to the present work.

© 2009 Elsevier B.V. All rights reserved.

1. Introduction

In all fusion plasma devices eroded surface materials are transported and redeposited on other locations, possibly far away from the point of origin. In devices like ITER, which will employ beryllium, tungsten and carbon on different plasma-facing surfaces, the formation of compound materials is highly probable. The properties of these compounds can differ significantly from the originally installed material: there may occur, e.g. drastic changes in melting points or greatly reduced erosion resistance. Therefore, it is likely that the newly formed compounds cannot meet the challenge posed by the surroundings, leading to a failure or deterioration of operation. On the other hand, in PISCES-B plasma simulator experiments it has also been observed that even a small fraction beryllium in the plasma tends to form a protective layer on carbon surfaces, thus mitigating the chemical erosion problem [1].

The present contribution is devoted to modelling mixed-material formation in an ITER-like environment. Arguably the only way to realistically simulate mixed-material effects is to include the interactions of the materials at the chemical level. To this end, we have used the molecular dynamics (MD) code HCParcas. On the other hand, modelling of the macroscopic migration of impurities requires a different approach. A well-established tool is the 3D Monte Carlo impurity transport code ERO [2] that consists of two main parts: a plasma–surface interaction part and an impurity transport part. Both parts use several physical models and var-

ious data sources. The original, so-called homogeneous material mixing surface model of ERO is, however, relatively simple and therefore not capable of describing reliably material mixing effects. Recently ERO has been coupled to the SDTrimSP code [3] for more realistic description of mixed layer formation on the surface. SDTrimSP can handle depth-resolved evolution of the surface and has been successfully benchmarked against experimental data. Since the code is based on the binary collision approximation, it has limited validity on impact energies below 100 eV.

An MD-based surface model can be implemented in ERO either by direct coupling, i.e., by simulating with HCParcas each particle impact during the ERO simulation, or generating in advance a sufficiently extensive interaction database for use in ERO simulations. Molecular dynamics is computationally very demanding and the resulting coupled code would have only marginal applicability. Therefore, we have run repeated simulations with the MD code to study the sputtering and reflection yields from an a-C:D surface during deuterium and carbon bombardment and implemented the resulting data in ERO. A previous ITER study was then repeated using these data. The progress in generating similar data for other ITER-relevant material combinations is reported in Ref. [4].

To understand the data needs of ERO, it is important to note that ERO distinguishes the traced impurities, ‘test particles’ and the ‘background plasma’ from each other. The effect of background plasma particles on the surface (physical sputtering and chemical erosion) is calculated from the known flux (e.g. from the SOLPS code). The effect of the increased impurity levels in the simulation volume is handled by launching impurity test particles, whose motion is followed in the electromagnetic fields, taking into account atomic and molecular processes and the effect of the background

* Corresponding author. Present address: VTT Technical Research Centre of Finland, P.O. Box 1000, FI-02044 VTT, Finland.

E-mail address: markus.airila@vtt.fi (M.I. Airila).

plasma. Test particle tracing yields information about the migration and redeposition of eroded impurities. In addition, the test particles represent the interaction of impurities with the surface. One can directly use sputtering yields for specific impact parameters for the test particles, whereas the background data must be averaged over the Maxwellian ion energy distribution and impact angle.

A more detailed description of our work can be found in Ref. [5].

2. New sputtering and reflection data

2.1. Molecular dynamics code HCParcas

For the MD simulations we used the HCParcas code, which is equipped with features especially tailored for hydrocarbon simulations. This is extremely important for fusion reactor conditions, where the chemical reactions of carbon play an essential role in the erosion, deposition and redeposition processes. The heart of the MD code is its potential model, which in the case of HCParcas is the empirical Brenner potential function for hydrocarbons [6]. The Brenner potential is a classical bond-order potential, allowing swift computation of interatomic forces and therefore imposes only moderate computational requirements on the simulation.

In addition, the Brenner potential is reactive, i.e., it describes bond breaking and forming, and it can thus be used to investigate chemical reactions. Another important observation is that it only requires one parameterization [7] to describe different phases of hydrocarbons. This feature is of great importance because it allows one to simulate transitions across different phases of carbon, such as melting or glass transitions in amorphous hydrocarbons.

For proper simulation of high-energy collisions, the equilibrium potential should be augmented by a ZBL one. In the current case the energies (maximum center-of-mass collisional energy of 75 eV) are only slightly above the validity range of the Brenner potential. Moreover, head-on-collisions are rare, so the maximum energy of validity of about 30 eV would only be rarely exceeded.

2.2. Simulation method

The data were collected by repeated simulations of single-atom bombardment on an $(18 \text{ \AA})^3$ amorphous deuterated carbon cell. The deuterium content was 30%, which corresponds roughly to the saturation level of hydrogen in graphite at room temperature, 0.4 H/C [8], and the sp^3/sp^2 ratio was 0.58. We ran the simulations using separately carbon and deuterium projectiles. For each incident energy, data were collected using six different surfaces and calculating 3000 impacts on every surface. The simulations were non-cumulative, i.e., the same intact surface was used again and again, but the impact location was randomized for every event by shifting the atoms periodically in the plane parallel to the surface. A cluster analysis was run after each impact to identify sputtered particles. The resulting sputtering yields are directly applicable to test particles in ERO simulations, while the data for background plasma erosion are obtained by an integration over energy and angle of incidence.

The present work covers only a narrow parameter range: normal incidence and six incident energies from 5 to 150 eV. The reason for extending the energy to such high energies (although our primary interest lies in low energies) is comparison to the present data set. The surface temperature was 300 K.

2.3. Carbon bombardment

2.3.1. Sputtering by test particles

We start with the calculation of sputtering yields and reflection probabilities of single impacting particles. ERO uses the Bohdanský formula [9]

$$Y(E_0, \alpha = 0^\circ) = Q s_n^{\text{KrC}}(\epsilon) \left(1 - \left(\frac{E_{\text{th}}}{E_0} \right)^{2/3} \right) \left(1 - \frac{E_{\text{th}}}{E_0} \right)^2, \quad (1)$$

supplemented by the Yamamura formula [10,11] for angular dependence, for calculating sputtering yields from test particle impacts. Here Q and E_{th} (threshold energy where the sputtering yield becomes zero) are fitting parameters, $\epsilon = E_0/E_{\text{TF}}$, where $E_{\text{TF}} = 5688 \text{ eV}$ is the Thomas–Fermi energy, and s_n^{KrC} is the nuclear stopping cross section based on the Kr–C potential, given by

$$s_n^{\text{KrC}}(\epsilon) = \frac{0.5 \ln(1 + 1.2288\epsilon)}{\epsilon + 0.1728\sqrt{\epsilon} + 0.008\epsilon^{0.1504}}. \quad (2)$$

In the original work of Bohdanský [9] the Thomas–Fermi nuclear stopping cross section was used instead of $s_n^{\text{KrC}}(\epsilon)$ [12].

The MD sputtering data averaged over the six sample surfaces are shown in Fig. 1. The sputtered species include both elemental carbon and hydrocarbons, the latter constituting about 2/3 of the sputtering yield. The hydrocarbon yield shows a similar energy dependence as the yield of atomic carbon, pointing to collisional energy transfer as the main release mechanism; therefore everything has been counted to physical sputtering. A detailed distinction between chemical and physical sputtering is beyond the scope of the current work, but can be achieved, e.g. with a combined analysis of the energy and ejection time of sputtered particles. For the current work it is sufficient to note that sputtered molecules are almost always formed by chemical sputtering, and sputtered individual atoms by physical sputtering. One should note that in the absence of simultaneous deuterium bombardment the continuous C bombardment would actually deplete the surface from deuterium. In order to interpret our result correctly one should therefore assume that enough deuterium is simultaneously incident to keep the concentration saturated.

The sputtering data can be conveniently implemented in ERO by fitting Eq. (1) to the data points using Q and E_{th} , resulting in values $Q = 0.642$ and $E_{\text{th}} = 8.56 \text{ eV}$. The original data set uses values $Q = 0.75$ and $E_{\text{th}} = 7.42 \text{ eV}$ (see Fig. 1).

It is worth noting that the sputtering yield is strongly influenced by the structure of the surface. In our modelling six different surfaces were used, which were obtained by opening one side of a cubic a-C:D sample at a time. One of these six surfaces features a several times higher sputtering yield in the form of hydrocarbons compared to the average of other five surfaces. Apparently there

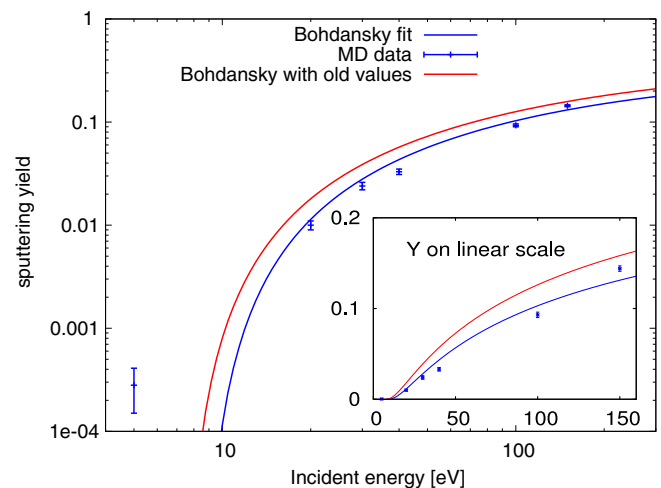


Fig. 1. The sputtering yield from MD simulations of carbon normally incident on a-C:D with different energies. The target contains 30% deuterium and has a temperature of 300 K. Old ERO data are also shown. Inset: The same data plotted on linear scale.

are loosely bound atoms on this surface which are easily sputtered time after time in our non-cumulative simulations. Concerning the validity of the MD data at higher energies, our simulation cell is sufficiently large up to about 100 eV. With 100 eV about 0.1% and at 150 eV about 0.5% of the incident particles impale the cell.

2.3.2. Sputtering by background plasma

ERO uses sputtering yields averaged over the Maxwellian ion energy distribution and an angular distribution to calculate the sputtering by the background plasma. The ion acceleration in the sheath potential is taken into account. In the implementation of MD data we have performed a similar averaging over the Maxwellian ion energy distribution and added the sheath contribution of $3ZkT_e$, but neglected the angular averaging due to the lack of angular data. This makes our new data less accurate than the old ERO data set – however, it does not affect our present simulations (see Section 3) in which beryllium is the only impurity in the background.

2.3.3. Carbon reflection

Although we get the reflection coefficient from the simulations, it is not useful to implement the data at this stage because of the strong dependence on the angle of incidence. Recall that we only have simulated normal incidence. In contrast, ERO uses a detailed description of reflection in which the reflection probability as well as the final energy and direction of the reflected particle are tabulated from TRIM data. However, it is interesting to compare our results to the corresponding values for normal incidence in this data set (Fig. 2). In the low-energy range, which is of primary interest to this work, there is a striking difference. While the TRIM data show zero reflection for low energies independently on the angle of incidence, in MD simulations the reflection probability increases as the incident energy approaches zero. The absolute values here ($\lesssim 4\%$) are small, but this behaviour would make a significant effect for non-normal incidence (as the reflection probability tends to increase with incidence angle). A more detailed investigation would be necessary in order to obtain an extensive data set for implementation in ERO.

3. ERO simulation results

We repeated the simulations reported in Ref. [13] and then changed the sputtering data (C on C) and the corresponding integrated data for background plasma sputtering. The results are

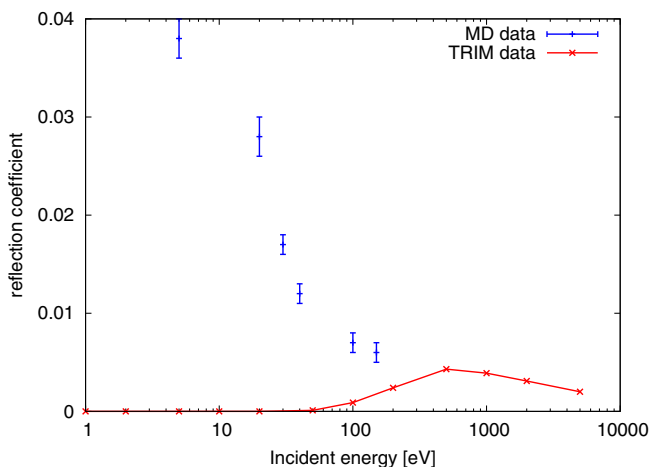


Fig. 2. Reflection coefficient of carbon incident on a-C:D with 30% D as a function of energy. The MD data are from the present work and the TRIM data are used in ERO. Normal incidence.

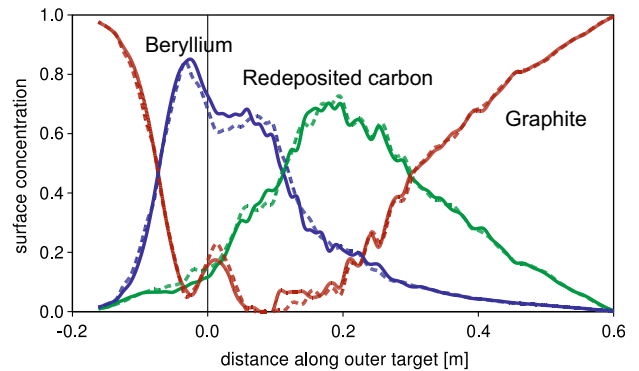


Fig. 3. Surface concentration profiles along outer divertor for graphite, redeposited carbon and beryllium. Solid lines correspond to the simulation with MD data and dashed lines to the reference simulation with old ERO data.

essentially same as in the original study. For instance, Fig. 3 shows the surface concentration profiles along the outer divertor for graphite, redeposited carbon and beryllium both with the original data set of ERO and with the new data. These profiles were chosen as an example since they are affected by all erosion and deposition processes and would therefore likely reveal any significant differences in erosion or deposition. The close agreement between simulations with different data sets was expected, since the change in test particle sputtering yield data set is small, and the averaged background plasma sputtering yield does not show up in the present case due to the absence of carbon impurities in the background. If a carbon-containing background is simulated, a more detailed angular averaging would be necessary. To this end, one either needs some more sputtering data with different angles of incidence or can resort to the Yamamura formula [10,11] for angular dependence.

4. Summary and discussion

Molecular dynamics has been considered for surface processes modelling in the ERO code. The method is accurate even at low ion energies where chemical effects become important and the binary collision approximation loses its validity. However, plasma-surface interactions involve slow processes whose time scales are out of reach of MD modelling. Important examples are the suppression of chemical erosion under high particle fluxes [14] and the diffusion of methane in solid matter. If such effects can be accounted for by other means, the MD method qualifies as a suitable candidate for PSI modelling in ERO. We have studied the feasibility of direct coupling of ERO and HCPParcs and concluded that simulations with the coupled code would become too heavy or only marginally feasible. For details, see Ref. [5].

One could proceed by generating an extensive particle-surface interaction database including the relevant elements. This would require at least about 100 surface concentration combinations of C/W/Be/D for a feasible accuracy and at least these four species as projectiles. Collecting the statistics for different energies and angles of incidence would correspond to several years of CPU time. However, the problem can be trivially parallelised. On the other hand, the generation of non-crystalline simulation cells requires much handwork, part of which could be replaced by generating the cells by cumulative bombardment of elemental cells. Use of this method could in fact result in more realistic compositions, including the depth-dependence of concentrations, which affects sputtering properties (see, e.g. [15]). In any case, a prerequisite for this work is that the interaction potentials between beryllium and all involved species – including beryllium itself – are available, see Ref. [4].

Our simulations show that carbon reflection at low impact energies is drastically different in MD and TRIM descriptions, a fact that requires a systematic study. Also an adequate description of chemical erosion requires some temperature variation instead of our present simulations at room temperature alone. Moreover, in most cases it would be more beneficial to carry out cumulative simulations with deuterium and impurities simultaneously incident on the surface. Re-use of simulation targets requires cooling the sample after each impact for some femtoseconds, which, however, does not essentially increase the total simulation time.

Acknowledgement

This work was carried out under the EFDA Task TW6-TPP-ERIT-ERB. Computing resources were provided by CSC the Finnish IT Center for Science.

References

- [1] R.P. Doerner, M.J. Baldwin, K. Schmid, Phys. Scr. T111 (2004) 75.
- [2] A. Kirschner, V. Philipps, J. Winter, U. Kögler, Nucl. Fusion 40 (2000) 989.
- [3] W. Eckstein, R. Dohmen, A. Mutzke, R. Schneider, SDTrimSP: A Monte Carlo code for calculating collision phenomena in randomized targets, IPP Report 12/3, Max-Planck-Institut für Plasmaphysik, 2007.
- [4] C. Björkas, N. Juslin, K. Nordlund, these proceedings.
- [5] M. Airila, T. Ikonen, Improvement of Surface Processes Modelling in the ERO Code for Advanced Description of Mixed Material Formation in ITER Reference Scenarios, Helsinki University of Technology Publications in Engineering Physics TKK-F-C200, Espoo, 2007.
- [6] D.W. Brenner, Phys. Rev. B 42 (1990) 9458.
- [7] K. Beardmore, R. Smith, Philos. Mag. A 74 (1996) 1439.
- [8] A.A. Haasz, P. Franzen, J.W. Davis, C. Chiu, C.S. Pitcher, J. Appl. Phys. 77 (1995) 66.
- [9] J. Bohdansky, Nucl. Instrum. and Meth. B 2 (1984) 587.
- [10] Y. Yamamura, Y. Itikawa, N. Itoh, Angular dependence of sputtering yields of monatomic solids, Report IPPJ-AM-26, Institute of Plasma Physics, Nagoya University, 1983.
- [11] U. Kögler, J. Winter, 3D-Monte Carlo code for local impurity-modeling in the scrape-off-layer of TEXTOR, Version 2.0, Report Jül-3361, Forschungszentrum Jülich, 1997.
- [12] C. García-Rosales, W. Eckstein, J. Roth, J. Nucl. Mater. 218 (1994) 8.
- [13] A. Kirschner, D. Borodin, S. Droste, V. Philipps, U. Samm, G. Federici, A. Kukushkin, A. Loarte, J. Nucl. Mater. 363–365 (2007) 91.
- [14] J. Roth et al., J. Nucl. Mater. 337–339 (2005) 970.
- [15] P.S. Krstic, C.O. Reinhold, S.J. Stuart, New J. Phys. 9 (2007) 209.